Journal of the European Ceramic Society **17** (1997) 1157–1166

PII: S0955-2219(96)00202-6
0955-2219/97/$17.00

Acoustic Studies of the Effect of SiC Particle Reinforcement on the Compaction of Alumina Powder

T. Kathrina* and R. D. Rawlings

Department of Materials, Imperial College of Science, Technology and Medicine, Prince Consort Road, London SW7 2BP, UK

(Received 9 May 1996; revised version received 12 September 1996; accepted 23 September 1996)

Abstract

A number of acoustic techniques namely, ultrasonic (US), acousto-ultrasonic (AU) and acoustic emission (AE), were employed to study the effect of reinforcement in the form of SiC particles on the compaction of spray-dried alumina powder. The US and AU techniques were shown to be capable of monitoring the processes occurring during loading and unloading, whereas AE could be used, in certain cases, to monitor the relative movement of particles in a powder compact during stress relaxation. The results were consistent with three stages of compaction, namely rearrangement of agglomerates, agglomerate breakdown and elastic deformation. The two pressure break-points between the stages, i.e. P_1 *and* P_2 *the pressures corresponding to the onset of breakdown of the agglomerates and to the change from permanent to elastic deformation, respectively, were determined by a number of different methods as a function of SiC content (10–40 vol%), type (equiaxed, angular or platelet) and size.*

1 Introduction

The early stage of ceramic processing can introduce defects which affect the quality of the final product. Consequently, monitoring of this stage is required in order to be able to reject a defective component before further processing, as early rejection of a defective component increases overall efficiency. Powder compaction is a forming technique often used in the early stage of ceramic processing and is the subject of this paper.

Studies of ceramic powder compaction previously undertaken have been mainly concerned with correlating the applied pressure to the packing density and investigating the mechanism of compaction.[1,2] Much of the work concentrated on determining a general compaction equation,[3–6] characterising the compaction behaviour of particulate material,[7] studying density-pressure distribution in a die[8,9] or observing effects of a binder and/or humidity on powder compaction.[10,11]

Acoustic non-destructive evaluation (NDE) techniques, namely ultrasonic testing (US), acousto-ultrasonics (AU) and acoustic emission (AE), which by definition do not damage the component under inspection, have the potential to monitor ceramic powders during compaction. The first of these techniques, US testing, involves measuring either the ultrasonic velocity or the attenuation of an elastic stress (acoustic) wave introduced into the material under interrogation. US studies of ceramics during powder compaction have been previously reported.[12–14]

AE technique is basically the monitoring of the emission of acoustic waves associated with a sudden source event on the surface or within the body of a material. Source events include plastic deformation and crack growth in solids, bursting of bubbles from gaseous corrosion products, and particle sliding and fracture of agglomerates in powders. In AE testing the stress waves are detected by a transducer and the resulting electrical signal may be processed and quantified in a number of ways to characterise the emissions, e.g. ringdown counting (RDC), amplitude distribution and frequency analysis.[15]

Acousto-ultrasonics (AU) consists of introducing a repeating series of ultrasonic pulses into the material under test and quantifying the output signal using AE methods. The output signal is

*Present address: P3FT-LIPI, Komplek PUSPIPTEK, Serpong, Tangerang 15314, Indonesia.

quantified in terms of the 'stress wave factor' (SWF) which is defined as a relative measure of the efficiency of energy dissipation in a material.[16] If flaws or other anomalies exist in the volume being examined, their combined effect will be reflected in the SWF value. The SWF in its simplest form may be evaluated by the AE parameters; ringdown count, peak-amplitude and pulse width. AU combines advantageous aspects of AE and US methodologies and alleviates some of their weaknesses, e.g. US is not very sensitive to highly attenuating materials and to dispersed small flaws and in AE testing a stress is often required to produce emissions and this may damage the material.

This paper is concerned with the use of the three acoustic techniques to monitor the compaction of spray-dried alumina powder and to determine the effect of the presence of reinforcement particles, in this case SiC, on the compaction process.

2 Experimental Procedure

The raw materials were a spray-dried alumina powder of spherical granule size in the range of 100–300 μm and with a particle size of 2–14 μm, and four SiC powders, designated batches A, B, C and D, with different particle shapes and size distributions as specified in Table 1. Each SiC batch was mixed with alumina powder in the following proportions: 10 vol%, 20 vol%, 30 vol% and 40 vol% SiC.

A compaction rig, which was designed to include transducers for acoustic monitoring, was constructed. It consisted of a pair of stainless steel rams located in a split cylindrical Perspex die which was held within a cylindrical brass sleeve (Fig. 1). A pair of broad band ultrasonic transducers (frequency range 175–1000 kHz, diameter 10 mm) were placed inside grooves in the rams and acoustically coupled by a thin layer of silicone grease.

Powder was placed between the rams and pressure was applied via a screw-driven Nene mechanical tester (capacity 100 kN). The applied load and the movement of the top plunger were recorded and the fractional volume compaction (V^*) at a given load was calculated from:[9]

$$V^* = \frac{V_0 - V_p}{V_0 - V_\infty} \tag{1}$$

V is the volume and the subscripts 0, p and ∞ refer to zero pressure, pressure P, and infinite pressure (corresponding to theoretical density) respectively. The die displacements were corrected to take into account the deflection of the rig system.

Acoustic monitoring was carried out while the crosshead was held stationary at various pressures from 5 MPa up to 120 MPa over two cycles of loading/unloading. For US and AU evaluation stress (acoustic) waves generated via the transmitting transducer were passed through the powder and were detected by the receiving transducer (Fig. 1). The signal from the latter was amplified, digitised and analysed by recording the ringdown count (RDC), amplitude (PA), pulse width (PW) and waveform. The US testing involved determining the ultrasonic velocity (v) by measuring the ultrasonic travel time (t) for propagation through the powder from the waveform. Knowing the compact thickness, s, the ultrasonic velocity was obtained from:

$$v = s/t \tag{2}$$

The stress wave factor from the AU measurements was quantified using the ringdown count, pulse amplitude and pulse width. At any particular load the results from 50 input pulses of constant amplitude were averaged. The pulse rate employed was 1 Hz. A total gain of 80 dB, a threshold of 30 dB and an envelope of 100 μs were used for ringdown count (RDC), amplitude (PA) and pulse width (PW) measurements, respectively. AU measurements were only made on powder mixtures from batches A and B due to a high level of intrinsic noise which appeared, even at low pressures, when compacting powders incorporating SiC from batches C and D. This intrinsic noise, or acoustic emission, was present during the periods when the crosshead was stationary and could not be separated from the AU signals. It was therefore decided to record the intrinsic AE signals using

Table 1. Size and shape of alumina and SiC particles

	Particle type				
	Al_2O_3	*SiC*			
		Batch A	*Batch B*	*Batch C*	*Batch D*
Particle size (μm)	2–14	3–11	6–34	8–55	50–150
Particle shape	–	Equiaxed, angular	Equiaxed, angular	Equiaxed, angular	Platelet

standard AE methodology during these periods to see whether they gave any insight into the compaction mechanisms in the powder mixtures made with batches C and D. The noise was monitored by recording the RDC, number of events and the peak amplitude distribution for 21 min. The total gain for RDC was adjusted to 90 dB and the threshold was held at 18 dB for the event and amplitude measurements. The small decrease in load that occurred during the 21 min that the crosshead was stationary was also recorded. Further experimental details may be found in Ref. 17.

3 Results

3.1 Ultrasonic testing

The results from the ultrasonic testing over two cycles of load compaction showed the velocity, v, and the fractional volume compaction, V^*, increased with pressure on first loading then decreased, almost linearly on unloading so that at low pressures both v and V^* were greater than on first loading. A typical set of results is presented in Fig. 2.

The effect of the proportion of SiC in the powder mixtures on v and V^* during first loading is shown in the graphs of Fig. 3. From these graphs it can be seen that an increase in volume fraction of SiC decreased both v and V^*.

It can be concluded from the results at constant SiC content (Fig. 4(a)), e.g. the 40 vol% SiC, that there is a general trend for mixtures containing equiaxed, angular particles from batches A, B and C for an increase of SiC particle size to lead to higher velocities at a given applied pressure. Batch D (platelets) additions tended to produce higher velocities than particles from the other batches. The effect of particle size on V^* (Fig. 4(b)) was not so well defined except that batch D usually had the higher values.

3.2 Acousto-ultrasonic

The AU versus pressure plots were similar for all the powder mixtures and are typified by the data for the 20 vol% SiC batch B presented in Fig. 5. On first loading the RDC and PW increased with increasing pressure but not smoothly as there were fluctuations in these parameters at pressure less than about 60 MPa. The pressure dependence of PA was similar to that of RDC and PW except that the fluctuations at low pressures were fewer in number and less marked.

The RDC and PW data for the first unloading and the second cycle of compaction were scattered around the first loading curve. In contrast, the PA values were lower than those for the first loading until the applied pressure reached 60 MPa, after which all PA values were similar.

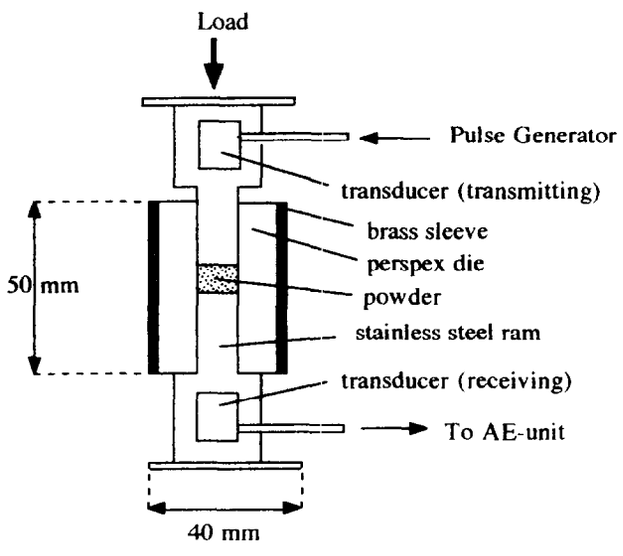

Fig. 1. Schematic diagram of compaction rig with acoustic monitoring facilities.

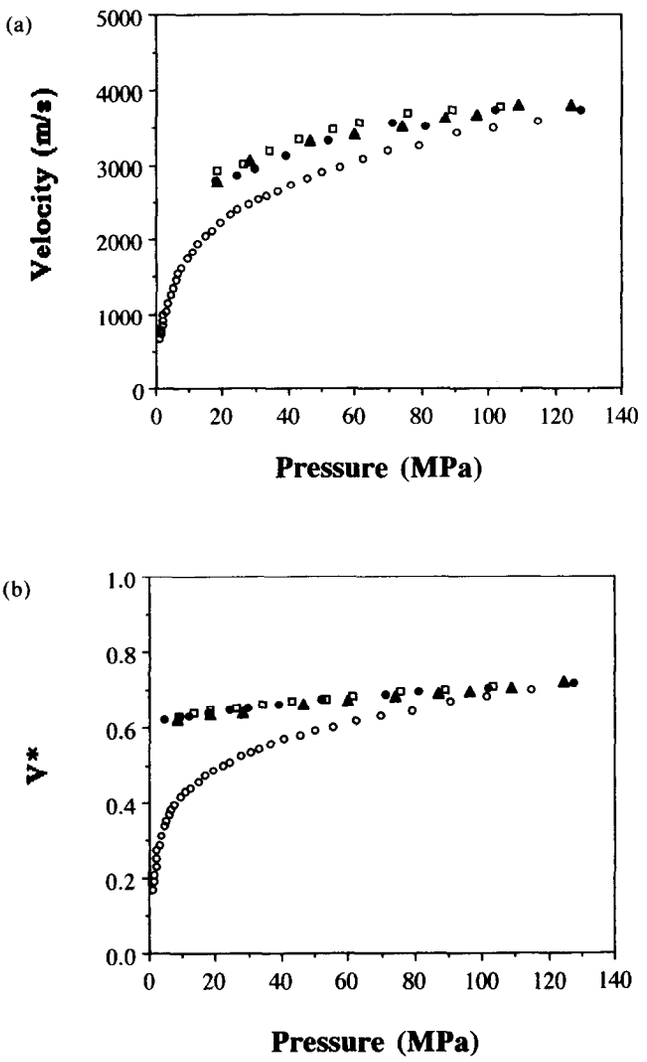

Fig. 2. Ultrasonic velocity (v) and fractional volume compaction (V^*) over two cycles of loading/unloading for powder mixture containing 20 vol% SiC of batch B; o first loading, ● first unloading, ▲ second loading, and □ second unloading.

The effect of powder mixture composition on the AU parameters was similar for all the SiC batches and hence only selected results for batch B are presented. The increase of reinforcement content in the mixture did not produce a regular change in RDC and PW though there was some tendency toward lower values with an increase of SiC content (Fig. 6). The SiC content has an even smaller effect on PA as shown by the curves of Fig. 7.

3.3 Acoustic emission

The ringdown and event counts recorded from the powder mixtures with SiC particles from batches C and D whilst the crosshead was stationary are exemplified by the results of Fig. 8. At a given pressure the RDC initially increased rapidly with time but the rate fell and eventually the RDC and the event count reached a constant value which was greater the higher the pressure.

Comparisons between samples with different SiC volume fraction (10–40 vol%) from the same batch, can also be made by plotting RDC against pressure (Fig. 9(a)) and number of event counts against pressure (Fig. 9(b)) for a given time of monitoring (in this case 21 min). Only batch D data are presented in these figures but results from both batches gave a linear relationship between the AE parameter and pressure for all samples with the slope being greater the higher the SiC content.

SiC type has an effect on the number of emissions recorded as demonstrated in Fig. 10. In terms of event count (Fig. 10(a)) batch C was noisier than batch D. In contrast the RDC plots for the two batches cross (Fig. 10(b)); batch D emitted more ringdown counts than batch C at higher pressures.

The peak amplitude distribution after 21 min at different initial pressures are presented in Fig. 11. The higher the pressure the greater was the number of events (as previously shown in Fig. 10(a)), but the peak amplitude range was the same

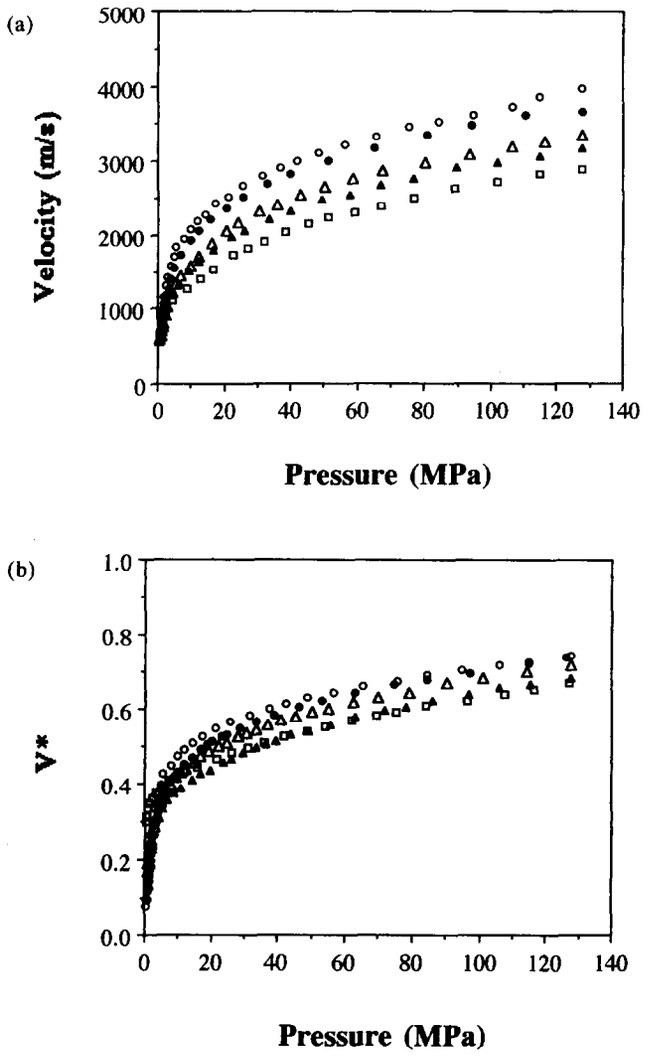

Fig. 3. Effect of SiC content on the pressure dependence of: (a) the ultrasonic velocity, and (b) the fractional volume compaction, during first loading cycle; e.g. batch A. ○ 0 vol% SiC, ● 10 vol% SiC, △ 20 vol% SiC, ▲ 30 vol% SiC, and □ 40 vol% SiC.

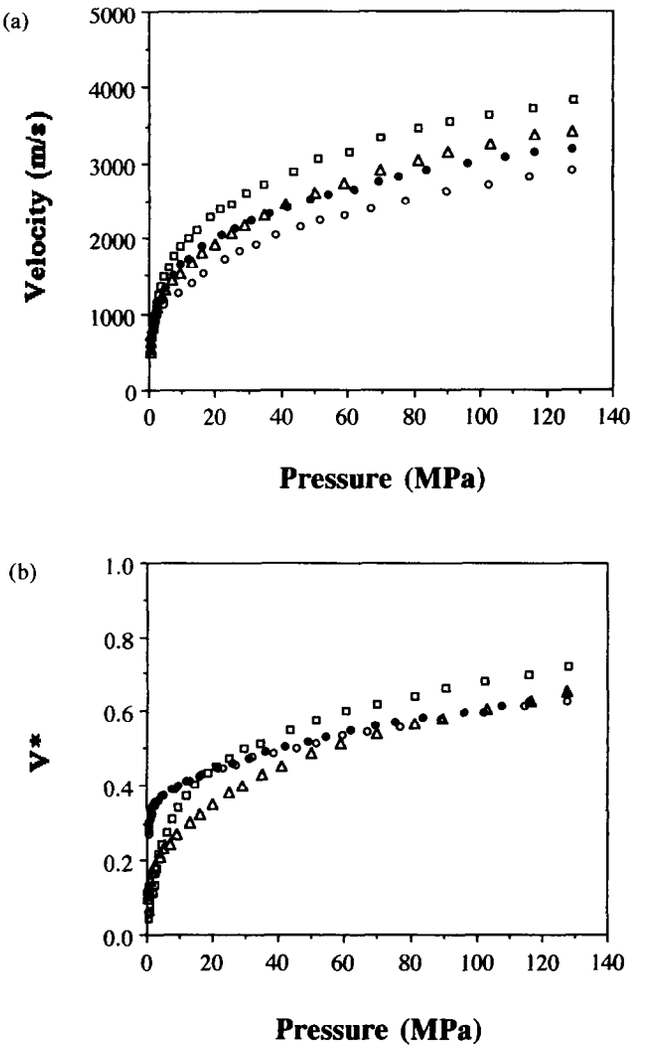

Fig. 4. Effect of shape and size (i.e. batch) of SiC on the pressure dependence of: (a) the ultrasonic velocity (v), and (b) the fractional volume compaction (V^*), during the first loading cycle: e.g. 40 vol% SiC. ○ batch A, ● batch B, △ batch C, and □ batch D.

irrespective of pressure, i.e. in the range of 10–40 dB for 20 vol% sample of batch C and 10–55 dB for the 40 vol% sample of batch D. For batch C the distribution was bimodal with a higher energy distribution appearing as a shoulder at about 28 dB on the more dominant lower energy distribution centred around 20 dB (Fig. 11(a)). The distributions for batch D were more complex and had the appearance of three superimposed subdistributions centred around 20, 28 and 38 dB. For both batches, but more noticeably for batch D, the higher energy subdistribution(s) increased relative to the 20 dB peak with increasing SiC content.

During the periods when the crosshead was held stationary in order to monitor the AE, it was found that the load decreased slightly due to relaxation processes in the equipment and the powder. Experiments demonstrated that the former was much smaller than the latter and that the relaxation of the powder could be readily obtained by subtracting the equipment relaxation from the total relaxation as shown in Fig. 12. There was a

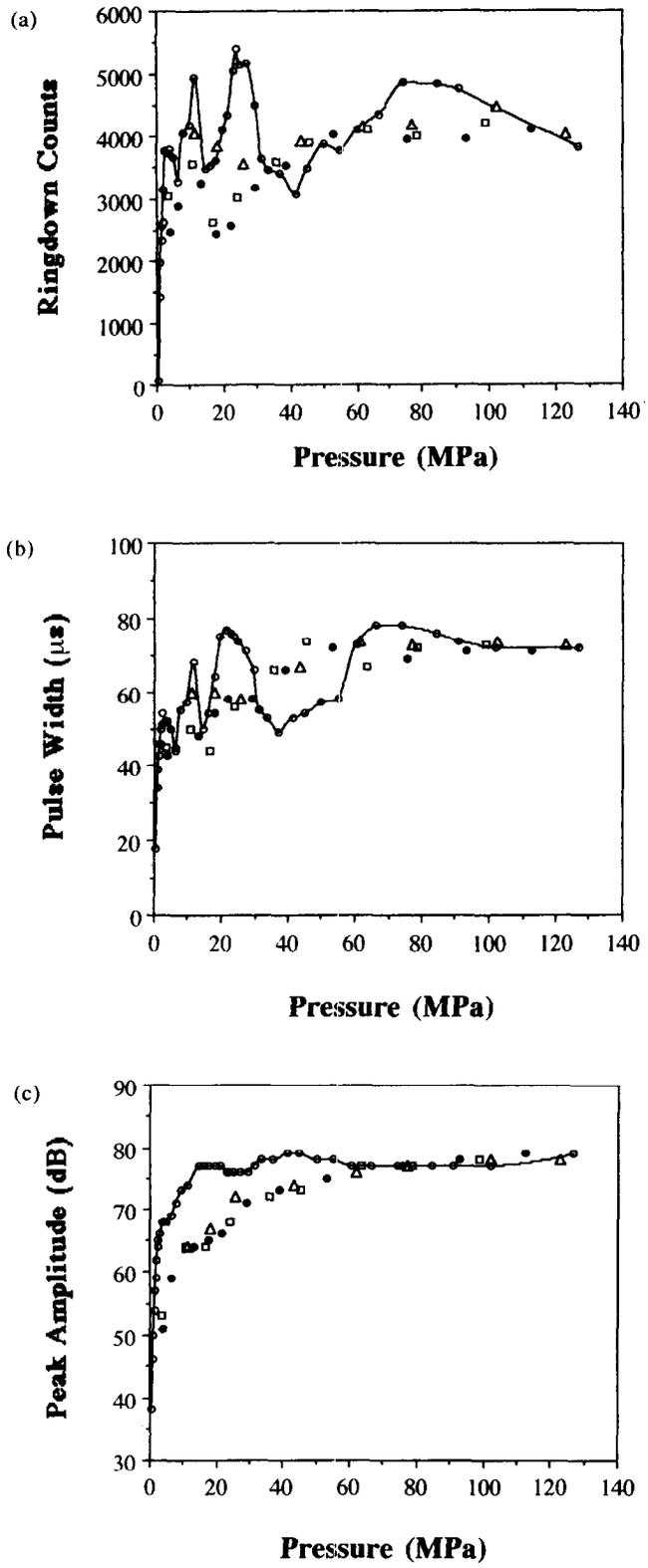

Fig. 5. Results from acousto-ultrasonic monitoring over two cycles of loading/unloading for powder mixture containing 20 vol% of batch B: (a) ringdown count (RDC), (b) pulse width (PW), (c) peak amplitude (PA). ○ first loading, ● first unloading, △ second loading, and □ second unloading.

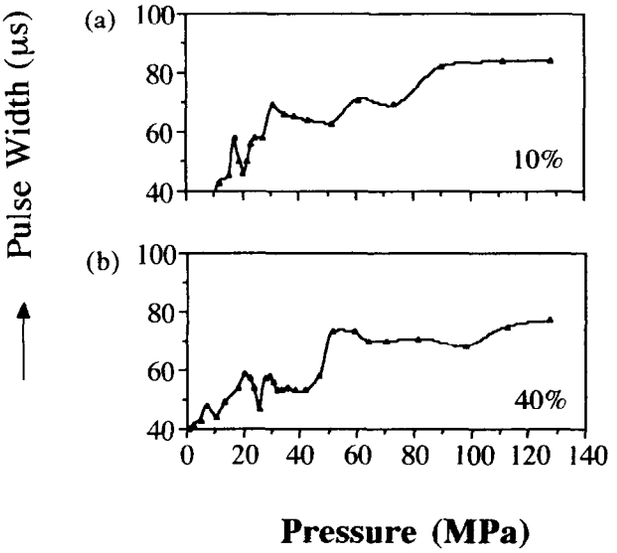

Fig. 6. Effect of SiC content on the pressure dependence of pulse width (PW) for powder mixtures containing batch B particles: (a) 10 vol% SiC, and (b) 40 vol% SiC.

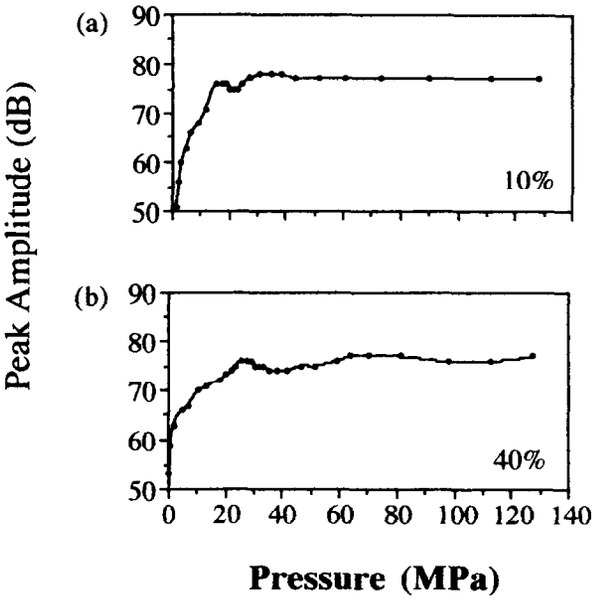

Fig. 7. Effect of SiC content on the pressure dependence of pulse amplitude (PA) for powder mixtures containing batch B particles: (a)10 vol% SiC, and (b) 40 vol% SiC.

general trend for the load decrement due to relaxation processes in the powder to increase with increasing initial pressure.

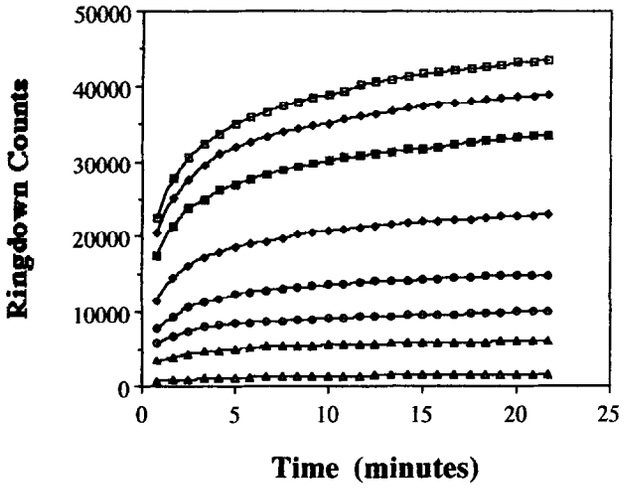

Fig. 8. Acoustic emission data for batch D in the form of ringdown count (RDC) as a function of time during the period the crosshead was held stationary at various initial pressures: ▼ 13 MPa, ▲ 25 MPa, ○ 38 MPa, ● 50 MPa, ◇ 64 MPa, ■ 76 MPa, ♦ 90 MPa, □ 102 MPa.

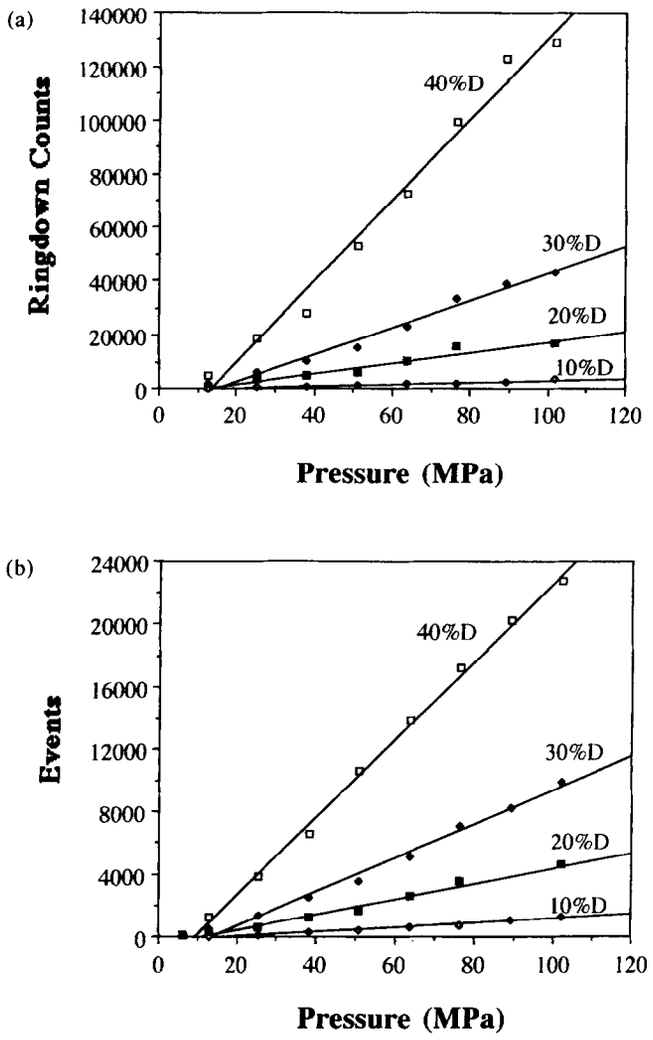

Fig. 9. Effect of SiC content (batch D) on the pressure dependence of acoustic emission (AE) parameters: (a) ringdown count (RDC) and (b) event count.

4 Discussion

4.1 Ultrasonic velocity and acousto-ultrasonic

During compaction the packing density increases and improves the bonding between particles. This allows the ultrasonic energy flow transfer in a material to increase with the increase of pressure. As a consequence the velocity and AU data increased with increasing pressure (e.g. Figs 2 and 5).

The lower velocities with increasing volume percentage of SiC (Fig. 3(a)) are due to the adverse effect that the reinforcement particles have on packing as shown by the data of Fig. 3(b). The same explanation accounts for the fact that an increase in SiC content tended to decrease the RDC and PW (Fig. 6). This is in agreement with previous work[18,19] on sintered glass matrix composites with SiC or Al_2O_3 reinforcement. However in the present work the PA remained approximately constant whereas in the sintered composites it decreased in a similar manner to RDC and PW. This was not observed in the present study; the

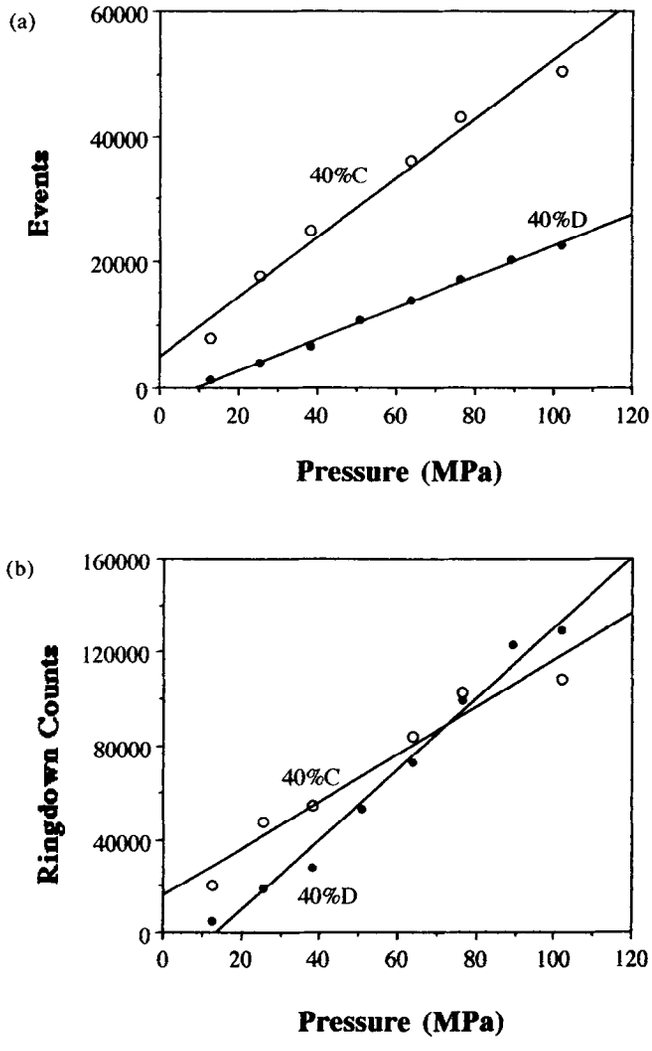

Fig. 10. Comparisons of (a) event count, and (b) ringdown count, from mixtures containing batch C (equiaxed angular) and batch D (platelet) SiC reinforcement as a function of pressure; e.g. 40 vol% SiC. ○ batch C, ● batch D.

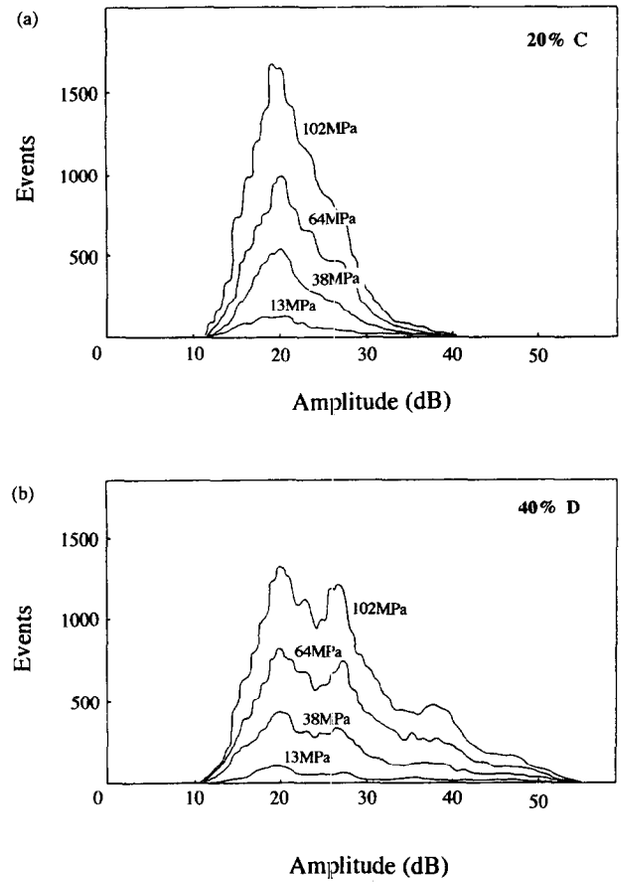

Fig. 11. Progress of peak amplitude distribution with pressure (a) 20 vol% batch C SiC and (b) 40 vol% batch D SiC.

reason for this difference in behaviour is unclear at present.

The increase in velocity with increase in average SiC particle size is attributed to the reduction in the total area of internal interfaces and, in the case of batch D powder mixtures, better contact between particles (Fig. 4).

4.2 Stages of powder compaction

There are three main stages in the compaction of ceramic powders: (i) rearrangement of agglomerates, (ii) permanent deformation by crushing of agglomerates and (iii) elastic deformation.[2,11,13] In this section a number of methods are used to determine the pressures at which the compaction mechanisms change.

During unloading the reduction in v and V^* is the consequence of reversible elastic, and perhaps inelastic deformation. Thus extrapolation of the unloading curves of Fig. 2 enables the pressure break point P_2 between the permanent and elastic stages of compaction to be determined. The results given in Table 2 show that the SiC content, size and morphology have no effect on P_2.

Plots of relative density D ($D = \rho/\rho_{the}$, where ρ_{the} is the theoretical density) have been used to characterise powder compaction[2] and have the generalised form of three straight lines which correspond to the different stages of compaction. The intersections of the lines give the pressure break points P_1, the pressure at which the agglomerates start to break down, and P_2. The break point values determined from such plots are given in Table 2. The values for P_2 are in good agreement with those obtained by the extrapolation method. The P_1 values show some scatter but it is clear that the equiaxed angular particles of batches A, B and C increase whereas the platelets of batch D decrease P_1 with respect to the alumina powder.

A compaction equation relating velocity v to the relative density D has recently been proposed by the authors[14,17] and was applied to the present data:

$$\log v = \frac{1}{2}\log\frac{E_o}{\rho_{the}} + \left(\frac{n-1}{2}\right)\log D \qquad (3)$$

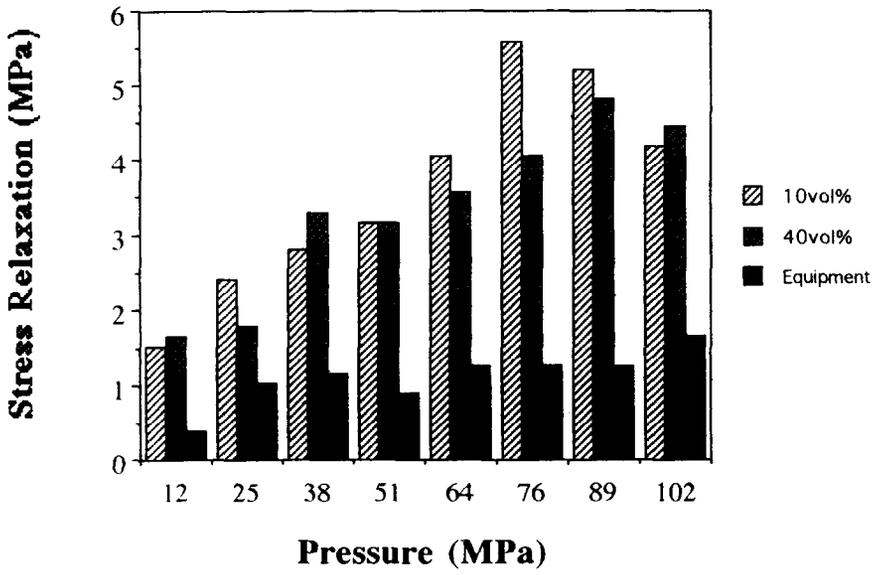

Fig. 12. Comparison of stress relaxation in the equipment and powder mixtures containing 10 vol% and 40 vol% batch D SiC after holding the crosshead stationary for 21 min.

Table 2. Pressure break points during compaction determined by three methods (U, extrapolation of first unloading data; *D–P*, *D* versus log (*P*); *v–D*, log (*v*) versus log (*D*))

	Pressure (MPa)						
	P_1				P_2		
	D–P	v–D	*Mean*	*U*	D–P	v–D	*Mean*
Alumina	4	4	4	60	60	60	60·0
Alumina + batch A SiC							
10 vol% SiC	4	10	7·0	50	60	60	56·5
20 vol% SiC	15	18	16·5	60	60	50	56·5
30 vol% SiC	15	12	13·5	65	50	50	55·0
40 vol% SiC	15	20	17·5	60	50	55	55·0
Alumina + batch B SiC							
10 vol% SiC	15	8	11·5	60	50	40	50·0
20 vol% SiC	18	15	16·5	60	60	60	60·0
30 vol% SiC	18	15	16·5	60	60	60	60·0
40 vol% SiC	15	15	15·0	—	60	60	60·0
Alumina + batch C SiC							
10 vol% SiC	15	6	10·5	60	60	35	51·5
20 vol% SiC	15	3	9·0	60	60	40	53·5
30 vol% SiC	12	3	7·5	60	60	50	56·5
40 vol% SiC	8	3	5·5	60	60	60	60·0
Alumina + batch D SiC							
10 vol% SiC	1	1	1·0	60	55	30	48·5
20 vol% SiC	1	2	1·5	60	60	45	55·0
30 vol% SiC	2	3	2·5	55	55	45	51·5
40 vol% SiC	2	3	2·5	55	50	50	51·5

E_0 is Young's modulus at zero porosity and n is the constant in the expression $E = E_0 (1-p)^n$ where p is porosity. Plots of log(v) against log(D) consisted of three linear regions corresponding to the three stages of compaction (Fig. 13). The intersections yielded values for D_1, v_1 and D_2, v_2 (the subscripts 1 and 2 indicate onset of agglomerate breakdown and onset of elastic stage, respectively) from which P_1 and P_2 were evaluated (Table 2). The P_1 and P_2 values are in reasonable agreement with those discussed previously with the exception of the slightly lower values for batch D.

Having identified the pressure break points it is possible to account for the fluctuations in the RDC and PW curves at pressures below about 60 MPa. These fluctuations are attributed to the rearrangement and breakdown of the agglomerates that occur during the permanent stages of compaction, i.e. up to pressure P_2. In these stages there is a significant change in the structure of the compact, especially of density, size and shape of the pores, and previous work by Aduda and Rawlings[20] has shown that the scattering of a signal is sensitive to the pore characteristics. This work indicated that velocity was determined solely by pore density in contrast to the AU parameters which depended also on pore size and shape. Thus the smooth velocity curves and the fluctuating AU curves suggest that the pore density decreases in a continuous manner whereas there are more sudden changes in shape and size of the pores.

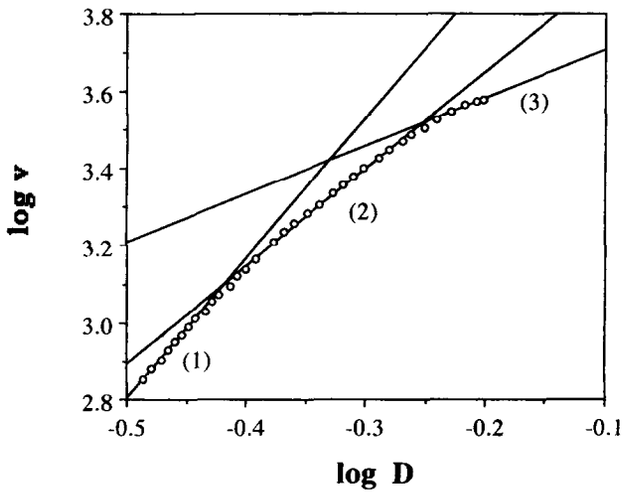

Fig. 13. Identification of the pressure break points P_1 and P_2 for alumina powder from a plot of log(velocity) against log(relative density).

4.3 Acoustic emission

The noise from the powder of batches C and D was attributed to deformation of the compact through continuing particle rearrangement under the approximately constant applied stress. The results demonstrate that the sudden rearrangements that are required to produce elastic stress waves only occur to a significant extent when large reinforcement particles are present. The noise may originate from alumina–alumina, SiC–SiC or alumina–SiC interactions; of these, the SiC–SiC are likely to be less frequent bearing in mind the size and volume fraction of the SiC particles. Friction between SiC particle and the Perspex sleeve wall was not expected to produce noise because of the high attenuation of Perspex. The dying out

of the acoustic events with time indicated that the particles rearranged to an equilibrium configuration commensurate with the relaxed applied stress on the compact. The higher the pressure the more extensive the movement of the particles, the more marked the interparticle interactions, and hence the greater the number of emissions (Fig. 8). The more extensive movement of the particles at higher pressures is consistent with the larger amounts of relaxation (Fig. 12) with increasing pressure. In fact, both the load decrement during relaxation and the AE parameters have a positive linear dependence on the applied pressure (Fig. 14). The greater propensity for noise with increase in the amount of SiC in a powder mixture (Fig. 9) is simply the consequence of more SiC particles acting as sources and is not due to changes in the amount of relaxation with SiC content.

Figure 10(a) shows that batch C produces more event counts than batch D whereas this is true for the RDC only in the lower pressure range (Fig. 10(b)). This difference in pressure dependence of the RDC and event count is due to differences in the energy of the events between the two batches. As demonstrated in Fig. 11, more high-energy events are recorded at high pressures for batch D and, as the number of RDC from an event depends on the energy, these high-energy events lead to many RDC for batch D at high pressures.

The complex amplitude distributions are the result of more than one source mechanism operating. The low amplitude peak (centred around 20 dB) is assigned to alumina–alumina interactions. The high amplitude peak (28 dB) is attributed to SiC–alumina interactions in batch C with approximately equiaxed particles. The particles in batch D are platelets and it is envisaged that the energy dissipated as elastic stress waves from an alumina particle interacting over a long distance on the large basal surface (50–150 μm) will be different to that associated with an interaction over a short distance with the edge (1–3 μm) of a platelet. Thus there are two high energy peaks centred around 28 and 39 dB for the platelet-containing powders.

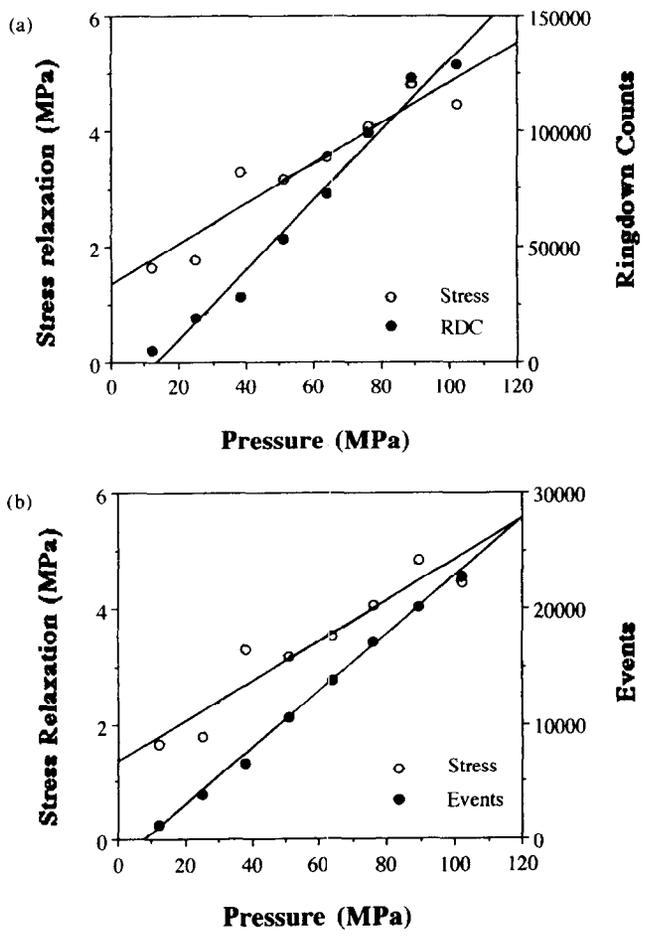

Fig. 14. Correlation between acoustic emission (AE) parameters and stress relaxation (due to the powder only) for 40 vol% batch D SiC: (a) ringdown count (RDC) and (b) event count.

5 Summary

Acoustic monitoring during the compaction of spray-dried alumina powders incorporating SiC reinforcement particles showed ultrasonic velocity and acousto-ultrasonic methods to give meaningful results which could be correlated with the different stages of compaction and the concomitant changes in pore structure. It was possible, for example, to determine the two pressure break points (P_1 and P_2) between the three stages of compaction.

Acoustic emission was found to be a sensitive NDE technique for monitoring the relative movement of particles in a compact during stress relaxation. The effects of applied pressure and SiC type and content could readily be detected.

Together these acoustic techniques are a powerful, yet relatively simple and inexpensive, means of investigating the behaviour of ceramic powders during compaction.

Acknowledgements

One of the authors (TK) gratefully acknowledges a grant from the Indonesia: BPP Technology Overseas Fellowship Programme. The authors thank Morgan Matroc Ltd for kindly supplying the alumina powder.

References

1. Lukasiewicz, S. J. and Reed, J. S., Character and compaction response of spray-dried agglomerates. *Ceram. Bull.*, 1978, **57**, 798–801.

2. Messing, G. L., Markhoff, C. J. and McCoy, L. G., Characterisation of ceramic powder compaction. *Ceram. Bull.*, 1982, **61**(8), 857–860.
3. Cooper, A. R. Jr and Eaton, L. E., Compaction behaviour of several ceramic powders. *J. Am. Ceram. Soc.*, 1962, **45**(3), 97–101.
4. Kawakita, K. and Ludde, K., Some considerations on powder compression equations. *Powder Technol.*, 1970, **4**, 61–68.
5. Cytermann, R. and Geva, R., Development of new model for compaction of powders. *Powder Metall.*, 1987, **30**, 256–260.
6. Ge, R., A new powder compaction equation. *Int. J. Powder Metall.*, 1991, **27**(3), 211–216.
7. Bruch, C. A., Problems in die-pressing submicron size alumina powder. *Ceramic Age*, October 1967, 44–53.
8. Huffine, C. L. and Bonilla, C. F., Particle-size effects in the compression of powders. *Am. Inst. Chem. Engng J.*, 1962, 490.
9. Leiser, D. B. and Whittemore, O. J. Jr, Compaction behaviour of ceramic particles. *Ceram. Bull.*, 1979, **49**, 714–717.
10. Brewer, J. A., Moore, R. H. and Reed, J. S., Effect of relative humidity on the compaction of barium titanate and manganese zinc ferrite agglomerates containing polyvinyl alcohol. *Ceram. Bull.*, 1981, **60**, 212–220.
11. Youshaw, R. A. and Halloran, J. W., Compaction of spray-dried powders. *Ceram. Bull.*, 1982, **61**, 227–230.
12. Jones, M. P. and Blessing, G. V., Ultrasonic studies of ceramic powders during compaction. In *International Advances in Non-destructive Testing*, vol. 13, ed. W. J. McGonnagle. Gordon and Breach, New York, 1988.
13. Kendall, K., Ultrasonic studies of ceramic powders during compaction. *Br. Ceram. Trans. J.*, 1990, **89**, 211–213.
14. Kathrina, T. and Rawlings, R. D., *Br. Ceram. Trans.* (accepted).
15. Raj, B. and Jha, B. B., Fundamentals of acoustic emission. *Br. J. NDT*, 1994, **36**(1), 16–23.
16. Vary, A., Acousto-ultrasonic characterization of fibre reinforced composites. *Mater. Eva.*, 1982, **40**, 650–654.
17. Kathrina, T., Non-destructive evaluation of ceramic processing using acoustic techniques. PhD thesis, Imperial College, London, 1994.
18. Aduda, A. O. B. and Rawlings, R. D., Acousto-ultrasonic testing of inorganic composites. Presented at 7th CIMTEC World Ceramic Congress, Montecatini Terme, Italy, 1990. Published by Elsevier.
19. Aduda, A. O. B., Monitoring of effect of inclusions in model glass systems using acousto-ultrasonic techniques. *Br. Ceram. Trans*, 1996, **95**, 10–14.
20. Aduda, A. O. B. and Rawlings, R. D., An acousto-ultrasonic study of the effect of porosity on a sintered glass system. *J. Mater. Sci.*, 1994, **29**, 2297–2303.